ISSN 0036-0244, Russian Journal of Physical Chemistry A, 2022, Vol. 96, No. 8, pp. 1637–1646. © Pleiades Publishing, Ltd., 2022.
Russian Text © The Author(s), 2022, published in Zhurnal Fizicheskoi Khimii, 2022, Vol. 96, No. 8, pp. 1118–1127.

CHEMICAL THERMODYNAMICS AND THERMOCHEMISTRY

Thermodynamic Properties of a Fourth-Generation Carbosilane Dendrimer with Terminal Trimethylsilylsiloxane Groups

N. N. Smirnova[a], A. V. Markin[a,*], S. S. Sologubov[a], S. A. Milenin[b], E. A. Tatarinova[b], and A. M. Muzafarov[b,c]

[a] *Lobachevsky State University, Nizhny Novgorod, 603105 Russia*
[b] *Enikolopov Institute of Synthetic Polymer Materials, Moscow, 117393 Russia*
[c] *Nesmeyanov Institute of Organoelement Compounds, Russian Academy of Sciences, Moscow, 119334 Russia*
**e-mail: markin@calorimetry-center.ru*

Received November 18, 2021; revised November 18, 2021; accepted January 6, 2022

Abstract—The heat capacity–temperature dependence for a fourth-generation carbosilane dendrimer with terminal trimethylsilylsiloxane groups is determined via adiabatic vacuum calorimetry in the 5–344 K range of temperatures and differential scanning calorimetry in the 310–560 K range of temperatures. An anomalous change in the heat capacity of the dendrimers in the range of $T = 46–68$ K is detected along with a transition in the range of $T = 179–196$ K, due to its devitrification. The thermodynamic characteristics of the detected transformations are determined and analyzed. The standard thermodynamic functions of the studied dendrimers in the range $T \to 0$ to 560 K and the standard entropy of its formation at $T = 298.15$ K are calculated using the obtained experimental data. A comparative analysis is performed of the thermodynamic properties of fourth-generation dendrimers that differ in the nature of their molecular skeletons and terminal groups.

Keywords: carbosilane dendrimers, precision calorimetry, heat capacity, devitrification, thermodynamic functions

DOI: 10.1134/S0036024422080210

INTRODUCTION

Dendrimers are nanosized spherical macromolecules characterized by monodisperse distributions (compared to classical polymers) and hyperbranched three-dimensional architectures. The main structural elements of dendrimers include a core (the initial multifunctional molecule), an inner sphere (exponentially repeating units resulting in the formation of G1, G2, G3, and higher generations), and an outer layer (terminal functional groups located on the surfaces of macromolecules and growing exponentially according to the number of the generation) [1–3].

Dendrimers are objects of intense fundamental and applied research, due to their highly ordered controlled structure and set of unique properties [4–8]. The precise geometry of macromolecules and the variability in the number of catalytic sites, which opens up new ways of controlling the mechanisms of chemical reactions, make dendrimers promising for use as catalysts [9, 10]. Dendrimers also have good solubility and biological inertness, so they can act as molecular containers for the targeted delivery of anticancer drugs. Results from biomedical studies of dendrimers are close to being put to use [11–14]. The development of materials for photonic and molecular electronics is based on dendrimers being an ensemble of macromolecules that is capable of self-assembly and resistant to chemicals, mechanical action, and photo oxidation [15–17].

Identifying a set of standard thermodynamic characteristics for dendrimers with different natures of their cores and surface layers via precision calorimetry in a wide range of temperatures allows us to establish and analyze relationships between compositions and structural properties that are of practical importance for these compounds [18–29]. Data on the thermodynamic properties of dendrimers serve as a theoretical basis in developing processes for preparing promising dendrimer-based nanomaterials.

The aim of this work was to perform a calorimetric study of a fourth-generation carbosilane dendrimer with terminal trimethylsilylsiloxane groups in the 5–560 K range of temperatures. It is a continuation of earlier studies to find the heat capacity of the dendrimer in the above range of temperatures; detect possible physical transformations and determine their thermodynamic characteristics; calculate the standard thermodynamic functions of the dendrimer in the range of $T \to 0$ to $T = 560$ K and the standard entropy of its formation from elementary substances at $T = 298.15$ K; and perform a comparative analysis of the thermodynamic properties of fourth-generation den-

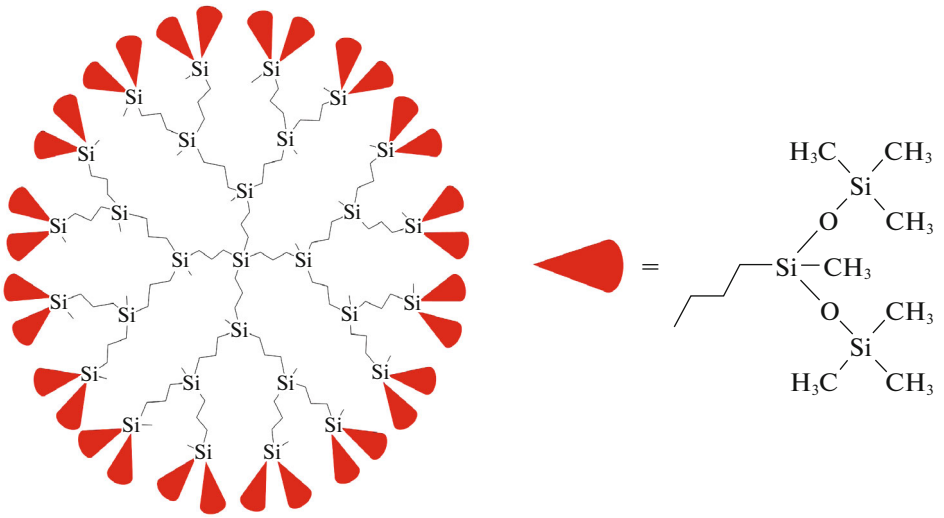

Fig. 1. Molecular structure of the fourth-generation carbosilane dendrimer with terminal trimethylsilylsiloxane groups $G4[OSi(CH_3)_3]_{64}$.

drimers that differ in the nature of their molecular skeletons and terminal groups.

EXPERIMENTAL

Sample Characteristics

Figure 1 shows the structure of the studied fourth-generation carbosilane dendrimers with terminal trimethylsilylsiloxane groups $G4[OSi(CH_3)_3]_{64}$, where G4 is the number of the generation of the dendrimer and $[OSi(CH_3)_3]_{64}$ denotes the fragment of the terminal groups of the dendrimer and their number. The sample was synthesized at the Enikolopov Institute of Synthetic Polymer Materials (Moscow, Russia). The polymer matrix for preparing the target dendrimer was a third-generation carbosilane dendrimer with terminal diallylmethylsilyl groups. Its outer layer was modified via hydrosilylation with Karstedt catalyst at room temperature. The modifier was 1,1,1,3,5,5,5-heptamethyltrisiloxane [30]. The composition and structure of the dendrimer were confirmed via elemental analysis, ^1H, ^{13}C, ^{29}Si NMR spectroscopy, and small-angle X-ray scattering. The intramolecular structure and macroscopic characteristics of the $G4[OSi(CH_3)_3]_{64}$ dendrimer were estimated by means of molecular dynamics using atomistic models. According to data from preparative-scale chromatography, the level of the main substance in the dendrimer was around 99 mol %. The molar weight of the $G4[OSi(CH_3)_3]_{64}$ carbosilane dendrimer ($M(C_{432}H_{1116}O_{64}Si_{125})$ = 10 848.1 g/mol) was calculated using the Table of Standard Atomic Weights as recommended by IUPAC [31].

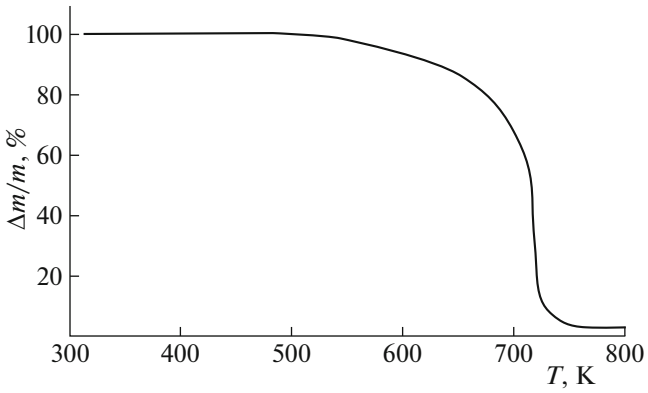

Fig. 2. Thermogravimetric curve for the fourth-generation $G4[OSi(CH_3)_3]_{64}$ carbosilane dendrimer; $\Delta m/m$ is the weight loss.

Apparatus and Measuring Procedure

Our thermogravimetric (TG) analysis of the $G4[OSi(CH_3)_3]_{64}$ carbosilane dendrimer was performed on a TG 209 F1 Iris thermobalance (NETZSCH, Germany) in the 300–800 K range of temperatures (purge gas, high-purity argon; gas flow rate, 25 mL min^{-1}). The weight of the dendrimer charge in an aluminum crucible was 17.653 mg; the crucible containing the substance was heated at a rate of 5 K min^{-1}. TG data showed that the initial decomposition temperature of the studied dendrimer was T = 560 K (weight loss, 2%). The resulting TG curve for the $G4[OSi(CH_3)_3]_{64}$ dendrimer is shown in Fig. 2.

The heat capacity–temperature dependence for the $G4[OSi(CH_3)_3]_{64}$ carbosilane dendrimer in the 5–344 K range of temperatures was determined using a BKT-3 adiabatic vacuum calorimeter (TERMIS, Russia). The design of the calorimeter and the measuring procedure were described in [32, 33]. Each sample of

the G4[OSi(CH$_3$)$_3$]$_{64}$ dendrimer (m = 0.1579 g) was weighed on a Shimadzu AUX 220 analytical balance (Japan) and placed in a titanium calorimetric ampule with thin walls. Prior to heat capacity measurements, small amounts of special purity dry helium gas (p ~ 5 kPa) were added to improve the heat conductivity of the calorimetric system. The cooling agents were liquid helium and nitrogen in the 5–85 and 83–344 K ranges of temperature, respectively. The rate of heating of the ampule containing the substance was 0.2 K min^{-1}. Calorimetric measurements were made twice in the temperature ranges where physical transformations of the dendrimer were observed. The reliability of the instrument was verified by measuring the heat capacities of reference samples of benzoic acid, synthetic sapphire, and high-purity copper in the 5–350 K range of temperatures [34]. The adiabatic calorimeter was found to allow determination of the heat capacities of compounds with relative expanded uncertainty $U_r(C_p) = 0.02$ in the 5–15 K range of temperatures, $U_r(C_p) = 0.005$ in the 15–40 K range of temperatures, and $U_r(C_p) = 0.002$ in the 40–350 K range of temperatures. The temperatures and enthalpies of phase and physical transformations were determined with standard uncertainty $u(T_{tr}) = 0.02$ K and cumulative relative expanded uncertainty $U_{c,r}(\Delta_{tr}H) = 0.01$, respectively.

The heat capacity of the G4[OSi(CH$_3$)$_3$]$_{64}$ carbosilane dendrimer in the 310–560 K range of temperatures was determined using a DSC 204 F1 Phoenix differential scanning calorimeter (NETZSCH, Germany). The experimental procedure and the design of the instrument were described in [35, 36]. The temperature and heat flow of the calorimeter were calibrated by determining the temperatures and enthalpies of melting of high-purity (99.99%) reference samples of indium, bismuth, tin, mercury, biphenyl, and cyclohexane [37]. The calibration experiments were performed at a heating rate of 5 K min^{-1}; the purge gas was high-purity argon with a flow rate of 25 mL min^{-1}. It was found that DSC allows the temperatures and enthalpies of phase and physical transformations to be determined with standard uncertainty $u(T_{tr}) = 0.5$ K and cumulative relative expanded uncertainty $U_{c,r}(\Delta_{tr}H) = 0.01$, respectively.

Determining the heat capacity via DSC required three successive measurements of [38]

• the baseline (a reference empty crucible + an empty crucible for each sample);

• a standard sample of α-Al_2O_3 sapphire (a reference empty crucible + a crucible with a sample of the sapphire);

• each considered sample (a reference empty crucible + a crucible with a sample of the dendrimer).

All DSC measurements were made in the 310–560 K range of temperatures at a heating rate of 5 K min^{-1} (purge gas, high-purity argon; gas flow rate, 25 mL min^{-1}). The weight of each G4[OSi(CH$_3$)$_3$]$_{64}$ dendrimer sample placed in an aluminum crucible for DSC measurements was 16.82 mg. The heat capacity of the dendrimer was determined according to ratios, according to the procedure described in the international ISO 11357-4:2021, ASTM E1269-11(2018), and DIN 51007:2019-04 standards. The resulting data were analyzed and processed using the NETZSCH Proteus Software program. DSC was found to allow determination of the heat capacities of substances with relative expanded uncertainty $U_r(C_p) = 0.02$ in the 310–560 K range of temperatures.

RESULTS AND DISCUSSION

Heat Capacity

The heat capacity–temperature curve for the G4[OSi(CH$_3$)$_3$]$_{64}$ carbosilane dendrimer is shown in Fig. 3. Experimental values of the dendrimer's heat capacity $C_{p,m}$ are given in Table 1 (Series 1–4 were obtained using an adiabatic vacuum calorimeter; Series 5 was obtained using DSC).

Standard Thermodynamic Characteristics of the Low-Temperature Heat Capacity Anomaly

The studied dendrimer was cooled from room temperature to the initial measuring temperature (T = 5 K) at a rate of 0.02 K s^{-1}. An anomalous change in the heat capacity of the sample was detected upon heating it in the range of T = (46–68) K (Fig. 4). The change was expressed as a positive deviation from the normal (interpolating) run of the curve. Similar anomalies were detected earlier in younger generations of carbosilane dendrimers with different terminal groups in the same range of temperatures. Such anomalies are systemic in nature. They are governed by the number of the dendrimer's generation, and are virtually independent of the nature of molecular skeleton and terminal groups. Combined calorimetric and spectral studies of several younger generations of dendrimers [18–21, 24–29] suggest that such transformations are due to thin structural (conformational) vibrations of methyl groups in dendrimer macromolecules when they are heated. As has been noted in the literature, such low-temperature anomalies should be attributed to equilibrium relaxation transitions of the order ⇄ disorder type, according to the Westrum–McCallaf thermodynamic classification.

Calculated thermodynamic characteristics of low-temperature anomalies of fourth-generation dendrimers are given in Table 2. The range of ΔT was determined from the heat capacity–temperature dependence. The points at which the anomalous heat capacity dependence starts and ends were taken as the

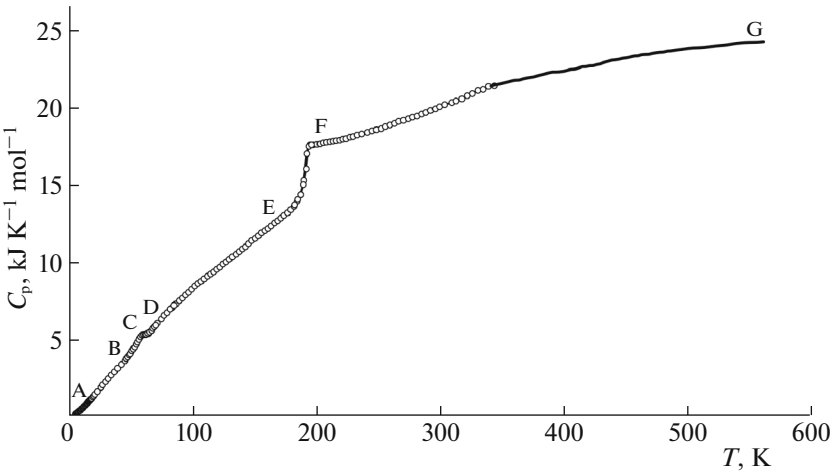

Fig. 3. Heat capacity of the fourth-generation G4[OSi(CH$_3$)$_3$]$_{64}$ carbosilane dendrimer as a function of temperature: AE is the amorphous (glassy) state, FG is the amorphous (devitrified) state, and BCD is the apparent heat capacity in the range of the low-temperature anomaly.

initial (T_{init}) and final (T_{fin}) temperatures of transition. Enthalpy $\Delta_{tr}H^\circ$ was calculated as the difference between integrals over curves $C_p^\circ = f(T)$ of apparent and normal heat capacities of the substance in the range of anomalies. Entropy $\Delta_{tr}S^\circ$ was calculated in a similar manner using the $C_p^\circ = f(\ln T)$ curve.

Standard Thermodynamic Characteristics of Devitrification and the Glassy State

The dendrimer is devitrified when heated in the range of T = (179–196) K (Fig. 3, BF section). The detected transition was reproduced upon cooling and reheating in the same range of temperatures.

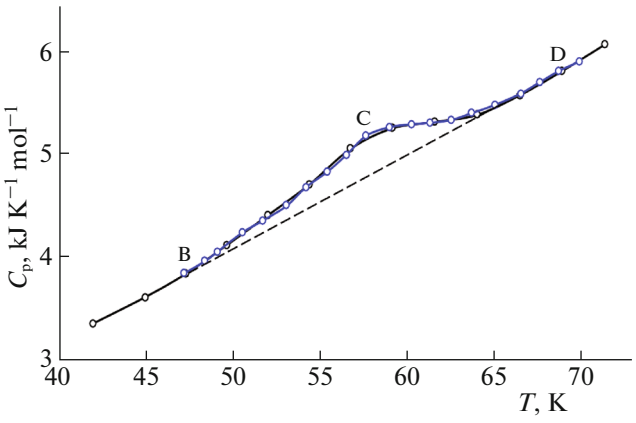

Fig. 4. Low-temperature anomaly of the heat capacity of the fourth-generation G4[OSi(CH$_3$)$_3$]$_{64}$ carbosilane dendrimer: BCD is the apparent heat capacity and BD (dashed line) is the normal (interpolating) run of heat capacity.

The thermodynamic characteristics of devitrification and the glassy state of the dendrimer include temperature T_g° of devitrification, range ΔT of the temperature of devitrification, change (increase) $\Delta C_p^\circ(T_g^\circ)$ in heat capacity upon devitrification, configurational entropy S_{conf}°, and residual entropy $S^\circ(0)$. Data obtained for the studied dendrimer and the available data for fourth-generation dendrimers are given in Table 3. Temperature T_g° of devitrification was defined as the point where three tangents to the $C_p^\circ = f(T)$ curve in the range of devitrification intersected. Range ΔT of devitrification and change $\Delta C_p^\circ(T_g^\circ)$ in heat capacity upon devitrification were determined graphically. Configurational entropy S_{conf}° was calculated according to the equation proposed in [39]:

$$S_{conf}^\circ = \Delta C_p^\circ(T_g^\circ)\ln(T_g^\circ/T_K), \quad (1)$$

where T_K is the Kauzmann temperature [40] and the (T_g°/T_K) ratio is 1.29 [41]. S_{conf}° was calculated by assuming the above ratio to be true for the studied compound. In determining the absolute entropy of the dendrimer, we assumed that $S_{conf}^\circ = S^\circ(0)$.

We may conclude from our comparative analysis of data obtained in this work and earlier that the temperature of dendrimer devitrification depends on both the chemical structure of the outer layer groups and the structure of the core. The temperature of devitrification was 176 K for the G4[OSi(CH$_3$)$_3$]$_{48}$ siloxane dendrimer with three branches from the central silicon atom (Fig. 5a). This low T_g° value was due to flexible siloxane fragments being in the inner sphere and on the surface layer of the dendrimer [29]. The studied fourth-generation carbosilane dendrimers had four branches from the central silicon atom, reducing their

Table 1. Experimental heat capacity values (kJ K^{-1} mol^{-1}) for the $G4[OSi(CH_3)_3]_{64}$ carbosilane dendrimer ($M(C_{432}H_{1116}O_{64}Si_{125})$ = 10848.1 g mol^{-1})

T, K	$C_{p,m}$	T, K	$C_{p,m}$	T, K	$C_{p,m}$	T, K	$C_{p,m}$	T, K	$C_{p,m}$	T, K	$C_{p,m}$
Series 1		41.98	3.360	93.91	7.878	208.30	17.80	193.97	17.52	433.5	23.0
5.13	0.143	44.98	3.616	96.44	8.061	210.97	17.82	196.12	17.61	436.5	23.0
5.33	0.156	47.31	3.842	98.97	8.244	213.63	17.85	Series 5 (DSC)		439.5	23.1
5.50	0.166	49.66	4.118	101.50	8.441	216.29	17.90	310.5	20.5	442.5	23.1
5.65	0.173	52.02	4.407	104.04	8.607	218.97	17.93	313.5	20.6	445.5	23.2
5.81	0.185	54.40	4.704	106.59	8.763	221.64	17.98	316.5	20.6	448.5	23.2
5.96	0.187	56.78	5.052	109.14	8.920	224.33	18.04	319.5	20.8	451.5	23.3
6.15	0.201	59.19	5.250	111.70	9.085	227.02	18.13	322.5	20.9	454.5	23.3
6.65	0.230	61.62	5.311	114.26	9.228	229.70	18.18	325.5	21.0	457.5	23.4
7.12	0.259	64.06	5.380	116.82	9.378	233.01	18.25	328.5	21.1	460.5	23.4
7.65	0.292	66.50	5.568	119.39	9.548	236.75	18.34	331.5	21.2	463.5	23.5
8.17	0.331	68.94	5.804	121.96	9.693	241.45	18.43	334.5	21.3	466.5	23.5
8.68	0.362	71.39	6.060	124.56	9.878	245.06	18.54	337.5	21.4	469.5	23.5
9.09	0.390	74.50	6.309	127.14	10.03	248.69	18.61	340.5	21.4	472.5	23.6
9.73	0.437	76.84	6.540	129.72	10.19	252.33	18.68	343.5	21.5	475.5	23.6
10.25	0.476	79.32	6.720	132.30	10.36	255.97	18.79	346.5	21.5	478.5	23.6
10.80	0.525	81.84	6.960	134.89	10.54	259.62	18.89	349.5	21.6	481.5	23.6
11.32	0.559	84.90	7.208	137.48	10.70	263.28	19.01	352.5	21.6	484.5	23.7
11.86	0.603	Series 2		140.08	10.86	266.95	19.13	355.5	21.7	487.5	23.7
12.31	0.646	46.02	3.745	142.67	11.01	270.62	19.21	358.5	21.8	490.5	23.8
12.85	0.687	47.22	3.848	145.27	11.21	274.30	19.33	361.5	21.8	493.5	23.8
13.32	0.729	48.41	3.966	147.87	11.41	277.97	19.41	364.5	21.8	496.5	23.8
13.85	0.777	49.12	4.057	150.48	11.55	281.65	19.49	367.5	21.9	499.5	23.8
14.33	0.821	50.56	4.242	153.09	11.72	285.32	19.61	370.5	21.9	502.5	23.9
14.82	0.867	51.72	4.356	155.70	11.90	288.98	19.71	373.5	22.0	505.5	23.9
15.23	0.9113	53.10	4.500	158.31	12.05	292.61	19.85	376.5	22.0	508.5	23.9
15.49	0.9373	54.21	4.679	160.93	12.20	296.34	19.96	379.5	22.1	511.5	23.9
15.88	0.9720	55.44	4.828	163.54	12.37	299.94	20.09	382.5	22.2	514.5	23.9
16.28	1.015	56.54	4.991	166.20	12.56	304.13	20.22	385.5	22.2	517.5	24.0
16.68	1.051	57.68	5.176	168.83	12.71	309.70	20.36	388.5	22.3	520.5	24.0
17.08	1.101	59.02	5.258	171.45	12.87	313.31	20.48	391.5	22.3	523.5	24.0
17.48	1.135	60.29	5.287	174.08	13.03	317.81	20.62	394.5	22.3	526.5	24.1
17.95	1.172	61.37	5.301	176.70	13.21	322.27	20.75	397.5	22.4	529.5	24.1
18.78	1.248	62.56	5.363	179.33	13.40	326.68	20.89	400.5	22.4	532.5	24.1
19.70	1.332	63.75	5.413	181.96	13.62	331.05	21.05	403.5	22.4	535.5	24.1
20.74	1.429	65.11	5.475	184.59	13.94	335.37	21.23	406.5	22.5	538.5	24.2
22.72	1.611	66.56	5.584	187.22	14.40	339.65	21.42	409.5	22.5	541.5	24.2
25.68	1.884	67.65	5.693	189.84	15.30	343.91	21.61	412.5	22.6	544.5	24.2
25.54	1.871	68.74	5.799	192.44	17.06	Series 4		415.5	22.7	547.5	24.3
27.03	2.024	69.94	5.894	195.04	17.62	182.25	13.72	418.5	22.7	550.5	24.3
29.57	2.255	Series 3		197.67	17.63	184.71	14.09	421.5	22.7	553.5	24.3
31.72	2.464	82.94	7.034	200.31	17.66	187.21	14.41	424.5	22.8	556.5	24.3
34.21	2.674	86.35	7.307	202.95	17.70	189.53	15.03	427.5	22.8	559.5	24.3
36.78	2.902	88.86	7.507	205.59	17.74	191.88	16.06	430.5	22.9	562.5	24.3
39.21	3.118	91.38	7.688								

The standard uncertainty was $u(T)$ = 0.02 K in the range of T = (5.13–343.91) K and $u(T)$ = 0.5 K in the range of T = (310.5–562.5) K. The relative expanded uncertainty was $U_r(C_{p,m})$ = 0.02, 0.005, 0.002, and 0.02 in the ranges of T = (5.13–14.82), (15.23–39.21), (41.98–343.91), and (310.5–562.5) K, respectively. The above uncertainties correspond to a confidence level of 0.95 ($k \approx 2$). Each third value of heat capacity is given for series 5 (DSC), and the $C_{p,m}$ values correspond to the devitrified state of the dendrimer.

Table 2. Standard thermodynamic characteristics of low-temperature heat capacity anomalies for fourth-generation dendrimers with different natures of the molecular skeleton and terminal groups

Dendrimer	ΔT, K	$\Delta_{tr}H^\circ$, J mol^{-1}	$\Delta_{tr}S^\circ$, J K^{-1} mol^{-1}	Reference
Carbosilane dendrimers				
G4[OSi(CH$_3$)$_3$]$_{64}$	46–68	2980	52.1	This work
G4[All]$_{64}$	56–70	3537	57.7	[18]
G4[But]$_{64}$	50–70	5997	81.6	[19]
Siloxane dendrimer				
G4[OSi(CH$_3$)$_3$]$_{48}$	43–65	1778	50.2	[29]

molecular mobility and raising their temperatures of devitrification relative to the siloxane dendrimer. Such a tendency was also observed for the G4[OSi(CH$_3$)$_3$]$_{64}$ dendrimer obtained in the this work (T_g° = 191 K), and for carbosilane dendrimer G4[But]$_{64}$ with terminal butyl groups (T_g° = 186 K) [19]. The liquid-crystalline fourth-generation dendrimer with terminal methoxyphenyl benzoate mesogenic groups G4[Und-MPhB]$_{64}$ had the highest temperature of devitrification (T_g° = 258 K) (Fig. 5b), which is explained by strong orientation interactions between them and thus the high rigidity of the dendrimer molecule in general [23]. The change in the chemical nature of the dendrimer molecular skeleton and surface layer is therefore an effective tool for controlling their different physicochemical characteristics.

Standard Thermodynamic Functions

The $C_p^\circ = f(T)$ curve was fitted using logarithmic polynomials and then extrapolated from the initial measurement temperature to $T \to 0$ using the Debye heat capacity function [42]

$$C_p^\circ = n\mathbf{D}(\Theta_\mathbf{D}/T), \quad (2)$$

where **D** is the Debye function and n = 83 and $\Theta_\mathbf{D}$ = 34.97 K are tailor-made parameters. Equation (2) with the above parameters describes the experimental C_p° values of the dendrimer in the range of T = (6–9) K with an error of ±1.3%.

The standard thermodynamic functions of the studied G4[OSi(CH$_3$)$_3$]$_{64}$ carbosilane dendrimer were calculated from the obtained values (Table 4) by assuming that Eq. 2 reproduces values with an error of ±1.3% when $T \le 6$ K. Enthalpy $[H^\circ(T) - H^\circ(0)]$ and entropy $[S^\circ(T) - S^\circ(0)]$ were calculated by numerically integrating functions $C_p^\circ = f(T)$ and $C_p^\circ = f(\ln T)$, respectively. Gibbs energy $[G^\circ(T) - H^\circ(0)]$ was calculated using the Gibbs–Helmholtz equation

$$[G^\circ(T) - H^\circ(0)] = [H^\circ(T) - H^\circ(0)] - T[S^\circ(T) - S^\circ(0)].$$

A detailed procedure for calculating standard thermodynamic functions was published in [43].

Using the values of $[S^\circ(T) - S^\circ(0)]$ at T = 298.15 K (Table 4) and the residual entropy for the studied dendrimer (Table 3) and the absolute entropies of elementary substances ($C_{(gr)}$, $H_{2(g)}$, $O_{2(g)}$, $Si_{(c)}$ [44]), we calculated the standard entropy of formation $\Delta_f S^\circ$ of the carbosilane dendrimer in the amorphous (devitrified)

Table 3. Standard thermodynamic characteristics of devitrification and the glassy state for fourth-generation dendrimers with different natures of the molecular skeleton and terminal groups

Dendrimer	ΔT, K	$(T_g^\circ \pm 1)$, K	$\Delta C_p^\circ(T_g^\circ)$, J K^{-1} mol^{-1}	$S_{conf}^\circ = S^\circ(0)$, J K^{-1} mol^{-1}	Reference
Carbosilane dendrimers					
G4[OSi(CH$_3$)$_3$]$_{64}$	179–196	191	3410	868	This work
G4[All]$_{64}$	170–180	172	3660	931	[18]
G4[But]$_{64}$	175–195	186	3820	973	[19]
Liquid-crystalline dendrimer					
G4[Und-MPhB]$_{64}$	230–275	258	15700	3998	[23]
Siloxane dendrimer					
G4[OSi(CH$_3$)$_3$]$_{48}$	157–187	176	1373	350	[29]

Table 4. Standard thermodynamic functions of the G4[$OSi(CH_3)_3$]$_{64}$ carbosilane dendrimer ($M(C_{432}H_{1116}O_{64}Si_{125})$ = 10848.1 g mol^{-1})

T, K	$C_p^\circ(T)$, kJ K^{-1} mol^{-1}	$[H^\circ(T) - H^\circ(0)]$, kJ mol^{-1}	$[S^\circ(T) - S^\circ(0)]$, kJ K^{-1} mol^{-1}	$-[G^\circ(T) - H^\circ(0)]$, kJ mol^{-1}
Glassy state				
5	0.132	0.182	0.0491	0.0637
10	0.457	1.62	0.2361	0.739
15	0.887	4.94	0.4992	2.55
20	1.360	10.59	0.8210	5.832
25	1.824	18.53	1.174	10.81
30	2.298	28.84	1.548	17.61
35	2.749	41.47	1.937	26.31
40	3.184	56.31	2.332	36.98
45	3.622	73.32	2.732	49.64
50	4.159	92.68	3.140	64.32
60	5.286	140.5	4.008	100.0
70	5.905	195.5	4.856	144.4
80	6.799	259.1	5.703	197.1
90	7.598	331.2	6.551	258.4
100	8.311	410.8	7.389	328.1
110	8.966	497.2	8.213	406.2
120	9.595	590.0	9.020	492.4
130	10.22	689.1	9.813	586.5
140	10.86	794.5	10.59	688.6
150	11.51	906.3	11.36	798.4
160	12.16	1025	12.13	915.8
170	12.80	1149	12.88	1041
180	13.41	1281	13.63	1173
190	14.05	1418	14.38	1314
191	14.11	1432	14.45	1328
Devitrified state				
191	17.52	1432	14.45	1328
200	17.66	1590	15.26	1462
210	17.80	1768	16.13	1619
220	17.97	1947	16.96	1784
230	18.18	2127	17.76	1958
240	18.40	2310	18.54	2139
250	18.65	2495	19.29	2328

Table 4. (Contd.)

T, K	$C_p^\circ(T)$, kJ K^{-1} mol^{-1}	$[H^\circ(T) - H^\circ(0)]$, kJ mol^{-1}	$[S^\circ(T) - S^\circ(0)]$, kJ K^{-1} mol^{-1}	$-[G^\circ(T) - H^\circ(0)]$, kJ mol^{-1}
260	18.91	2683	20.03	2525
270	19.19	2874	20.75	2729
280	19.48	3067	21.45	2940
290	19.77	3263	22.14	3158
298.15	20.02	3425	22.69	3341
300	20.07	3462	22.82	3383
310	20.39	3665	23.48	3614
320	20.73	3870	24.13	3852
330	21.07	4078	24.77	4097
340	21.39	4290	25.41	4348
350	21.60	4506	26.0	4605
360	21.8	4723	26.6	4868
370	21.9	4942	27.2	5138
380	22.1	5162	27.8	5413
390	22.2	5384	28.4	5694
400	22.4	5607	29.0	5981
410	22.6	5832	29.5	6274
420	22.7	6058	30.1	6572
430	22.9	6286	30.6	6875
440	23.1	6516	31.1	7184
450	23.2	6748	31.7	7498
460	23.4	6981	32.2	7817
470	23.5	7215	32. 7	8141
480	23.6	7451	33.2	8470
490	23.8	7688	33.7	8805
500	23.9	7926	34.1	9144
510	23.9	8165	34.6	9487
520	24.0	8405	35.1	9836
530	24.1	8645	35.5	10189
540	24.2	8887	36.0	10546
550	24.2	9129	36.4	10909
560	24.3	9371	36.9	11275

The standard uncertainties were $u(p) = 10$ kPa, $u(T) = 0.01$ K in the temperature range of 5–350 K, and $u(T) = 0.5$ K in the temperature range of 350–560 K. The cumulative expanded relative uncertainties were $U_{c,r}(C_p^\circ(T)) = 0.02$, 0.005, 0.002, and 0.02; $U_{c,r}([H^\circ(T) - H^\circ(0)]) = 0.022$, 0.007, 0.005, and 0.022; $U_{c,r}([S^\circ(T) - S^\circ(0)]) = 0.023$, 0.008, 0.006, and 0.023; $U_{c,r}([G^\circ(T) - H^\circ(0)]) = 0.03$, 0.01, 0.009, and 0.03 in the temperature ranges of 5–15, 15–40, 40–350, and 350–560 K, respectively. The above uncertainties correspond to a confidence level of 0.95 ($k \approx 2$).

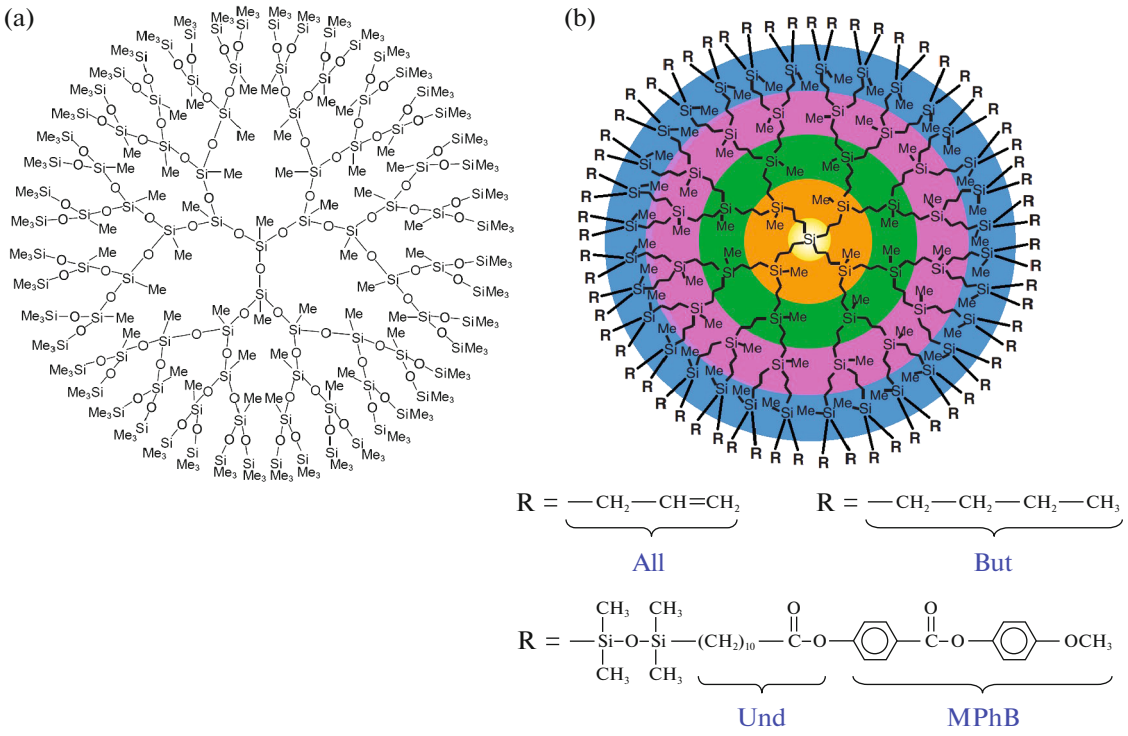

Fig. 5. Molecular structures of the fourth-generation (a) siloxane and (b) carbosilane dendrimers with different terminal functional groups.

state at the same temperature. Resulting value $\Delta_f S°(C_{432}H_{1116}O_{64}Si_{125}, 298.15) = -60699 \pm 298$ J K^{-1} mol^{-1} corresponds to the equation

$$432C_{(gr)} + 558H_{2(g)} + 32O_{2(g)} + 125Si_{(c)} \rightarrow C_{432}H_{1116}O_{64}Si_{125(dev)},$$

where (gr) is graphite, (g) is gas, (c) is crystal, and (dev) is the devitrified state.

FUNDING

This work was supported by the RF Ministry of Science and Higher Education as part of State Task no. 0729-2020-0053; and by the Russian Foundation for Basic Research, project no. 19-03-00248.

CONFLICT OF INTEREST

The authors declare they have no conflicts of interest.

REFERENCES

1. *Dendrimers and Other Dendritic Polymers,* Ed. by J. M. J. Fréchet and D. A. Tomalia (Wiley, Chichester, UK, 2001).
2. G. R. Newkome, C. N. Moorefield, and F. Vögtle, *Dendrimers and Dendrons: Concepts, Syntheses, Applications* (Wiley-VCH, Weinheim, 2002).
3. F. Vögtle, G. Richardt, and N. Werner, *Dendrimer Chemistry: Concepts, Syntheses, Properties, Applications* (Wiley-VCH, Weinheim, 2009).
4. A. W. Bosman, H. M. Janssen, and E. W. Meijer, Chem. Rev. **99**, 1665 (1999).
5. D. A. Tomalia, Prog. Polym. Sci. **30**, 294 (2005).
6. A. M. Muzafarov and E. A. Rebrov, J. Polym. Sci. A **46**, 4935 (2008).
7. L. M. Bronstein and Z. B. Shifrina, Chem. Rev. **111**, 5301 (2011).
8. A. M. Muzafarov, N. G. Vasilenko, E. A. Tatarinova, G. M. Ignat'eva, V. M. Myakushev, M. A. Obrezkova, I. B. Meshkov, N. V. Voronina, and O. V. Novozhilov, Polymer Sci., Ser. C **53**, 48 (2011).
9. R. van Heerbeek, P. C. J. Kamer, P. W. N. M. van Leeuwen, et al., Chem. Rev. **102**, 3717 (2002).
10. D. Astruc, E. Boisselier, and C. Ornelas, Chem. Rev. **110**, 1857 (2010).
11. S. Svenson and D. A. Tomalia, Adv. Drug Deliv. Rev. **57**, 2106 (2005).
12. M. A. Mintzer and M. W. Grinstaff, Chem. Soc. Rev. **40**, 173 (2011).
13. J. Yang, Q. Zhang, H. Chang, et al., Chem. Rev. **115**, 5274 (2015).
14. E. Pędziwiatr-Werbicka, K. Milowska, V. Dzmitruk, et al., Eur. Polym. J. **119**, 61 (2019).
15. M. J. Cho, D. H. Choi, P. A. Sullivan, et al., Prog. Polym. Sci. **33**, 1013 (2008).
16. W. Wu, C. Ye, J. Qin, et al., ACS Appl. Mater. Interfaces **5**, 7033 (2013).

17. X. Zhang, Y. Zeng, T. Yu, et al., J. Phys. Chem. Lett. **5**, 2340 (2014).
18. B. V. Lebedev, M. V. Ryabkov, E. A. Tatarinova, et al., Russ. Chem. Bull. **52**, 545 (2003).
19. N. N. Smirnova, O. V. Stepanova, T. A. Bykova, et al., Thermochim. Acta **440**, 188 (2006).
20. N. N. Smirnova, A. V. Markin, Ya. S. Samosudova, G. M. Ignat'eva, E. Yu. Katarzhnova, and A. M. Muzafarov, Russ. J. Phys. Chem. A **87**, 552 (2013).
21. A. V. Markin, S. S. Sologubov, N. N. Smirnova, et al., Thermochim. Acta **617**, 144 (2015).
22. S. S. Sologubov, A. V. Markin, N. N. Smirnova, et al., J. Phys. Chem. B **119**, 14527 (2015).
23. Ya. S. Samosudova, A. V. Markin, N. N. Smirnova, et al., J. Chem. Thermodyn. **98**, 33 (2016).
24. S. S. Sologubov, A. V. Markin, N. N. Smirnova, et al., J. Therm. Anal. Calorim. **125**, 595 (2016).
25. N. N. Smirnova, S. S. Sologubov, Yu. A. Sarmini, A. V. Markin, N. A. Novozhilova, E. A. Tatarinova, and A. M. Muzafarov, Russ. J. Phys. Chem. A **91**, 2317 (2017).
26. S. S. Sologubov, A. V. Markin, N. N. Smirnova, N. A. Novozhilova, E. A. Tatarinova, and A. M. Muzafarov, Russ. J. Phys. Chem. A **92**, 235 (2018).
27. S. S. Sologubov, A. V. Markin, Yu. A. Sarmini, et al., J. Therm. Anal. Calorim. **138**, 3301 (2019).
28. A. V. Markin, Yu. A. Sarmini, S. S. Sologubov, N. N. Smirnova, K. L. Boldyrev, E. A. Tatarinova, I. B. Meshkov, and A. M. Muzafarov, Russ. J. Phys. Chem. A **94**, 240 (2020).
29. S. S. Sologubov, A. V. Markin, Yu. A. Sarmini, et al., J. Chem. Thermodyn. **153**, 106318 (2021).
30. S. A. Milenin, E. V. Selezneva, P. A. Tikhonov, et al., Polymers **13**, 606 (2021).
31. J. Meija, T. B. Coplen, M. Berglund, et al., Pure Appl. Chem. **88**, 265 (2016).
32. V. M. Malyshev, G. A. Mil'ner, E. L. Sorkin, et al., Prib. Tekh. Eksp., No. 6, 195 (1985).
33. R. M. Varushchenko, A. I. Druzhinina, and E. L. Sorkin, J. Chem. Thermodyn. **29**, 623 (1997).
34. R. Sabbah, A. Xu-wu, J. S. Chickos, et al., Thermochim Acta **331**, 93 (1999).
35. G. W. H. Hohne, W. F. Hemminger, and H.-J. Flammersheim, *Differential Scanning Calorimetry* (Springer, Heidelberg, 2003).
36. P. Gabbott, *Principles and Applications of Thermal Analysis* (Blackwell, Oxford, UK, 2008).
37. G. della Gatta, M. J. Richardson, S. M. Sarge, et al., Pure Appl. Chem. **78**, 1455 (2006).
38. E. Kaisersberger, J. Janoschek, and E. Wassmer, Thermochim. Acta **148**, 499 (1989).
39. G. Adam and J. H. Gibbs, J. Chem. Phys. **43**, 139 (1965).
40. W. Kauzmann, Chem. Rev. **43**, 219 (1948).
41. A. B. Bestul and S. S. Chang, J. Chem. Phys. **40**, 3731 (1964).
42. P. Debye, Ann. Phys. (N.Y.) **344**, 789 (1912).
43. *Experimental Thermodynamics,* Vol. 1: *Calorimetry of Non-Reacting Systems,* Ed. by J. P. McCullough and D. W. Scott (Butterworth, London, 1968).
44. M. W. Chase, J. Phys. Chem. Ref. Data **1–2,** 1951 (1998).

Translated by K. Utegenov